cmgh
CELLULAR AND MOLECULAR GASTROENTEROLOGY AND HEPATOLOGY

RESEARCH LETTER

Spontaneous Cholemia in C57BL/6 Mice Predisposes to Liver Cancer in NASH

C57BL/6 mice are widely used for metabolic, cancer, and immunologic studies. High-caloric diets induce a heterogeneous phenotype in C57BL/6 mice, with the majority developing obesity and metabolic syndrome, while others remain lean and metabolically healthy.[1] Western diets (WDs), methionine-deficient or choline deficient–based diets are used to study nonalcoholic fatty liver disease and nonalcoholic steatohepatitis (NASH), important risk factors for hepatocellular carcinoma development.[2–4]

When conducting metabolic studies with NASH-inducing diets, we found several mice remained lean but developed liver cancer at time points at which previously only NASH had been reported.[5,6] These mice showed increased markers of biliary damage (serum total bile acids [TBA] and alkaline phosphatase [ALP]). To understand the link between these serum parameters and accelerated liver cancer development, we segregated mice before NASH-diet feeding and followed them up prospectively (Figure 1*A* and *B*).

Screening male C57BL/6J littermates from Janvier Labs (Le Genest-Saint-Isle, France) at 6 weeks of age identified a heterogeneous serum TBA pattern (Figure 1*C*). Mice showing serum TBA levels greater than 45 μmol/L (9.1%) were classified as cholemic/high-TBA (H-TBA) (Figure 1*C*), because complications caused by increased serum TBA only occur at levels greater than 40–45 μmol/L.[7,8] Cholemia was corroborated in C57BL/6J mice from Jackson Laboratories (Bar Harbor, ME) (14.6%) and Charles River Laboratories (Margate, UK) (23.8%) (Supplementary Figure 1*A* and *B*). Importantly, cholemia was not observed in either B6-FVB/N-129 or DBA/2 mice (Supplementary Figure 1*C* and *D*).

Next, mice were fed either standard chow or a WD (Figure 1*D*). Chow feeding caused no accelerated liver cancer phenotype in either low-TBA (L-TBA) or H-TBA mice (data not shown). H-TBA mice lacked any differences in body weight before WD feeding compared with L-TBA mice (Figure 1*E*). H-TBA mice showed accelerated and increased liver damage (serum alanine aminotransferase, ALT; ALP) upon WD feeding (Figure 1*F* and *G*). H-TBA WD-fed mice showed significantly lower levels of serum cholesterol compared with WD L-TBA mice, likely owing to the requirement of cholesterol for bile acid synthesis (Figure 1*H*). H-TBA, WD-fed mice remained lean throughout the experiment and showed improved glucose homeostasis and serum triglyceride levels (Figure 1*I* and *J*, Supplementary Figure 1*E–K*).

At 32 weeks after starting the diet, the H-TBA, WD-fed mice retained higher liver damage (serum ALT and ALP) and showed liver cancer with 100% penetrance (Figure 1*K–P*, Supplementary Figure 1*L*). Thus, H-TBA/cholemic mice show metabolic improvements at the expense of accelerated liver cancer. Histologic analyses showed tumor nodules of different sizes in WD-fed, H-TBA mice, with loss of collagen IV and increased hepatocyte proliferation, indicative of hepatocellular carcinoma (Figure 2*A*, Supplementary Figure 2*A*). H-TBA mice showed profound biliary expansion, higher fibrosis, yellow coloration of the serum, and increased serum total bilirubin levels (Figure 2*B–F*). Although livers of H-TBA mice showed biliary expansion, none of the tumors were of biliary origin (cytokeratin 19 - CK19), while showing positivity for the hepatocyte marker hepatocyte nuclear factor 4 alpha (HNF4A) (Supplementary Figure 2*A*). In addition, H-TBA mice fed a WD showed significantly higher immune cell infiltrates (Supplementary Figure 2*B–F*). Notably, the exacerbated liver damage in H-TBA mice was evident at as early as 5 weeks of WD feeding (Supplementary Figure 3*A* and *B*).

We observed no consistent differences in expression of genes involved in bile acid synthesis or transport between H-TBA and L-TBA mice fed a WD (Supplementary Figure 3*C*). TBA levels remained strongly increased in H-TBA, WD-fed mice at 32 weeks after starting the diet (Figure 2*G*), primarily owing to taurine conjugates (taurocholic acid and tauro-β-muricholic acid) and unconjugated cholic acid (Supplementary Figure 3*D*). Previous reports have shown that taurocholic acid is not only a predictive biomarker of cirrhosis but also drives liver cirrhosis.[9] Here, serum TBA and ALP levels strongly correlated with increased liver fibrosis (Figure 2*H* and *I*).

RNA sequencing of liver homogenates from L-TBA and H-TBA mice fed a WD showed a clear separation between groups (Figure 2*J*). Gene ontology and gene set enrichment analysis indicated increased fibrosis and proliferation as well as activation of the Notch and mitogen-activated protein kinase pathways (Figure 2*K* and *L*, Supplementary Figure 3*E*). Gene set enrichment analysis also showed enrichment for the Yes-associated protein signature in H-TBA mice (Figure 2*L*), supporting previous findings showing that bile acids activate Yes-associated protein to promote carcinogenesis.[10]

The accelerated liver cancer phenotype in H-TBA cholemic mice was corroborated using an alternate WD with high trans-saturated fats or a choline-deficient high-fat diet (Supplementary Figure 4*A–D*). In addition, cholemic female mice also developed accelerated liver cancer upon WD feeding (data not shown). Nevertheless, cholemic mice did not show exacerbated liver damage to the

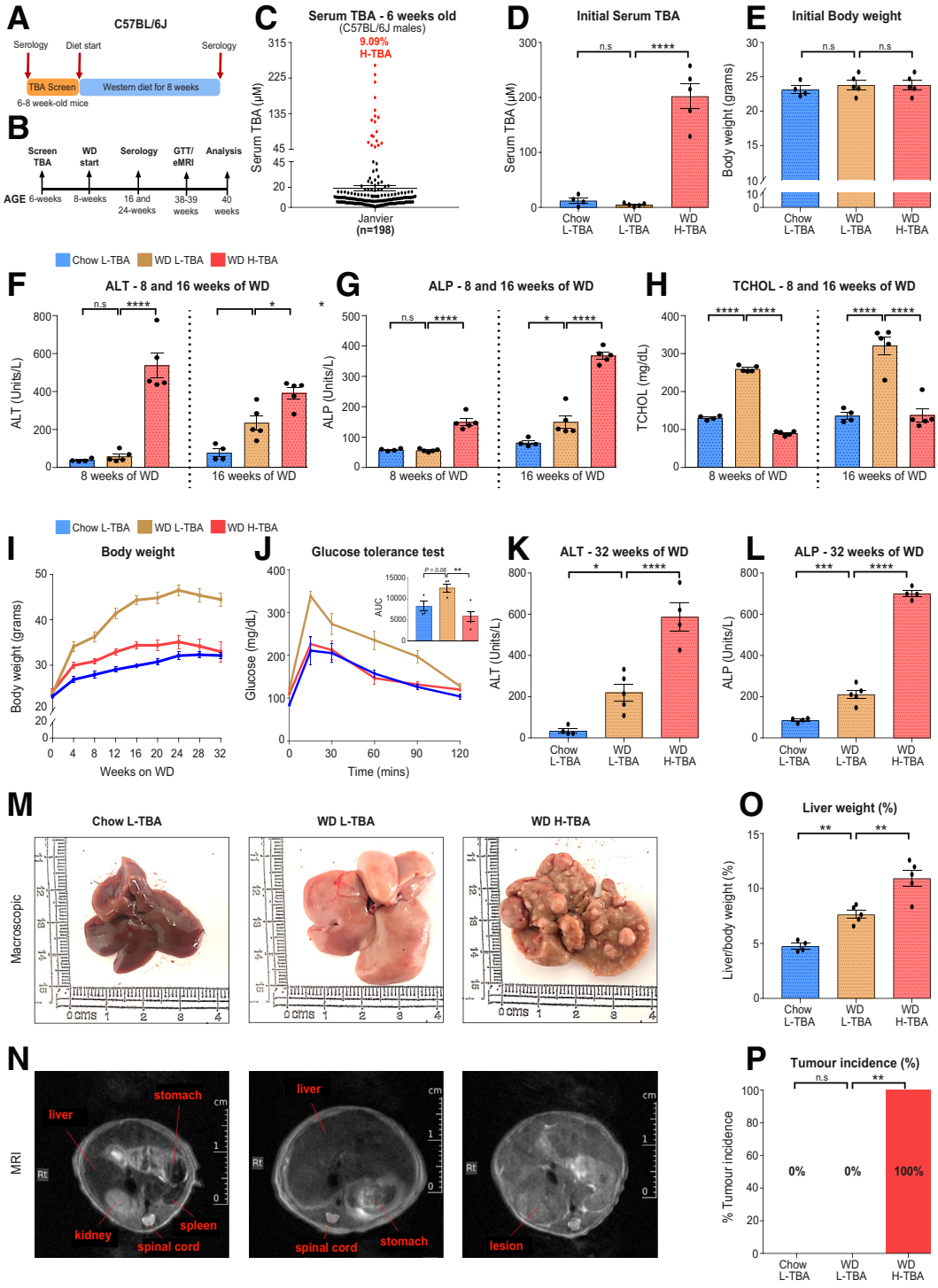

Figure 1. Spontaneous cholemia in C57BL/6 mice upon Western diet feeding. (*A*) Proposed protocol for screening of cholemic mice. (*B*) Experimental scheme. (*C*) Serum TBAs from 6-week-old C57BL/6J Janvier Labs mice. L-TBA (<45 µmol/L) or H-TBA (≥45 µmol/L). (*D*) Serum TBA before diet feeding. (*E*) Initial body weight measurement. (*F–H*) Serum alanine aminotransferase (ALT), ALP, and cholesterol levels. (*I*) Body weight development. (*J*) Intraperitoneal glucose tolerance test after 30 weeks of diet. (*K* and *L*) Serum ALT and ALP levels. (*M*) Liver images. (*N*) Magnetic resonance imaging (MRI) scans of livers after 30 weeks of diet. (*O*) Liver to body weight ratio (%). (*P*) Liver tumor incidence. Chow L-TBA, n = 4 mice; WD L-TBA, n = 5 mice; WD H-TBA, n = 5 mice. Data are expressed as means ± SEM. Statistical significance was calculated using either 1-way analysis of variance with the (D-H, J-L– and *O*) Tukey multiple comparison test or the (*P*) Fischer exact test. **P* < .05, ***P* < .01, ****P* < .001, and *****P* < .0001. eMRI, echoMRI; GTT, glucose tolerance test.

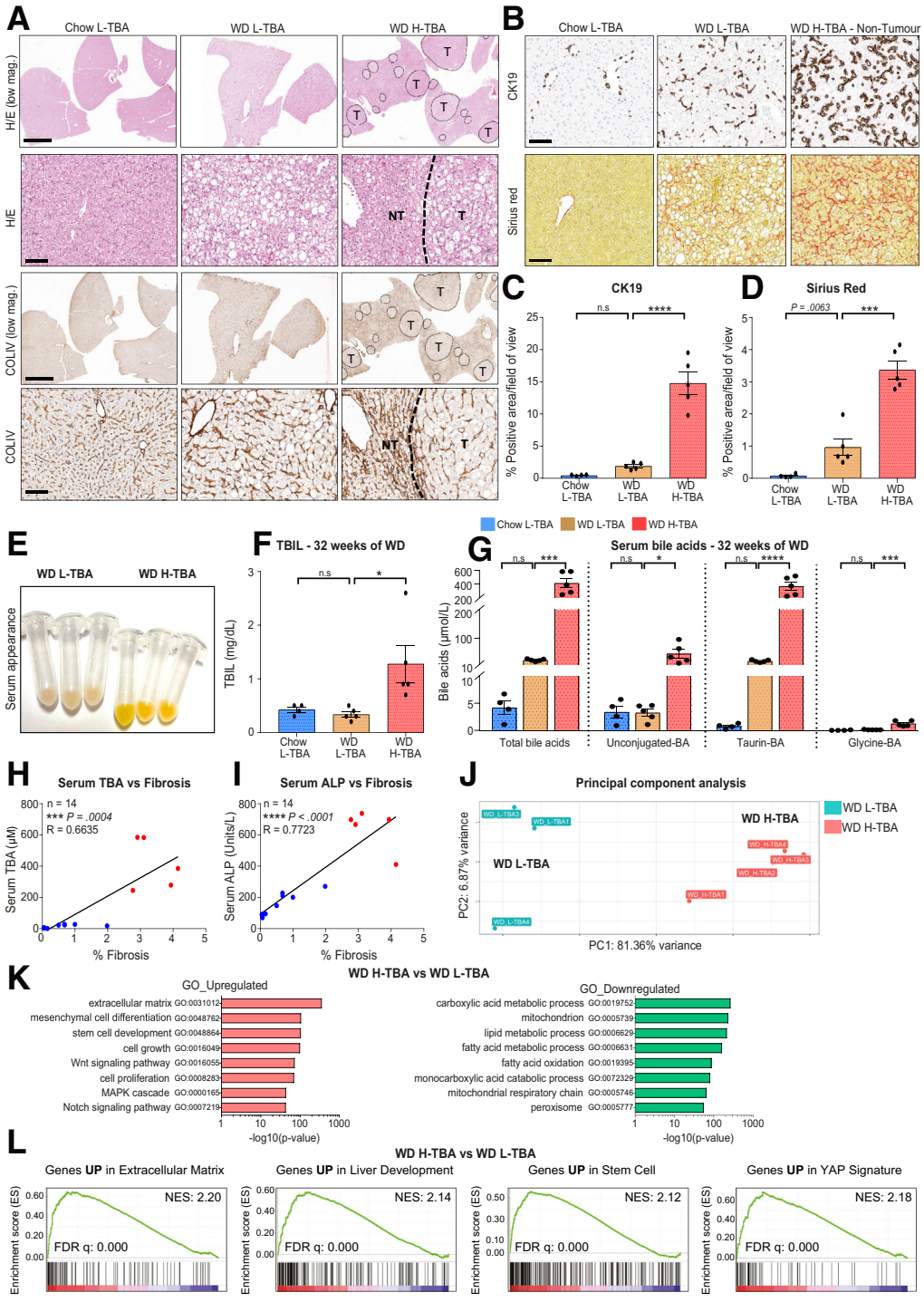

Figure 2. Cholemic mice show exacerbated biliary damage, liver fibrosis, and up-regulation of proliferative pathways upon Western diet feeding. (*A*) H&E and collagen IV (COLIV) staining of livers; *dashed line* indicates the tumor (T) border. *Scale bars*: 1 mm (low magnification) and 100 μm. (*B*) Cytokeratin 19 (CK19) and Sirius red staining. *Scale bar*: 100 μm. (*C*) Quantification of CK19 and (*D*) Sirius red–positive area. (*E*) Serum appearance. (*F*) Serum total bilirubin (TBIL) levels. (*G*) Serum TBA profiling. (*H* and *I*) Correlation plots. (*J*) Principal component analysis, (*K*) gene ontology (GO) analysis, and (*L*) gene-set enrichment analysis of H-TBA mice compared with L-TBA mice fed a WD. (*A–I*) Chow L-TBA n = 4; WD L-TBA n = 5; WD H-TBA n = 5 mice. (*J–L*) WD L-TBA n = 3; WD H-TBA n = 4 mice. Data are expressed as means ± SEM. Statistical significance calculated by 1-way analysis of variance with the (*C*, *D*, *F*, and *G*) Tukey multiple comparison test or (*H* and *I*) linear regression. $^{*}P < .05$, $^{***}P < .001$, $^{****}P < .0001$. FDR, false discovery rate; MAPK, mitogen-activated protein kinase; NES, normalized enrichment score; NT, non-tumor.

well-characterized CCl_4-induced model of liver fibrosis (Supplementary Figure 4*E–G*). This suggests that cholemia-induced accelerated liver damage and cancer may be specific to high-caloric feeding.

Overall, a subset (5%–25%) of all C57BL/6 mice, obtained from different commercial breeders, develop spontaneous cholemia, predisposing them to liver cancer upon high-caloric feeding. The molecular and genetic basis for development of spontaneous cholemia in C57BL/6 mice remains to be investigated. We suggest that future metabolic and liver cancer studies should screen C57BL/6

mice for TBA and exclude cholemic mice to prevent inconsistent or perplexing findings.

SUCHIRA GALLAGE[*]
ADNAN ALI[*]
JOSE EFREN BARRAGAN AVILA
Division of Chronic Inflammation and Cancer
German Cancer Research Center (DKFZ)
Heidelberg, Germany

DIRAN HEREBIAN
Department of General Pediatrics
Neonatology and Pediatric Cardiology
Medical Faculty
University Hospital Düsseldorf
Heinrich Heine University
Düsseldorf, Germany

MOHAMMAD M. KARIMI
Comprehensive Cancer Centre
School of Cancer and Pharmaceutical Sciences
Faculty of Life Sciences and Medicine
King's College London
Denmark Hill, London, United Kingdom

ELAINE E. IRVINE
DOMHNALL MCHUGH
Medical Research Council (MRC) London Institute of Medical Sciences
London, United Kingdom
Institute of Clinical Sciences
Faculty of Medicine
Imperial College London
London, United Kingdom

ANNE T. SCHNEIDER
MIHAEL VUCUR
VERENA KEITEL
Department of Gastroenterology
Hepatology and Infectious Diseases
Medical Faculty
University Hospital Düsseldorf
Heinrich Heine University
Düsseldorf, Germany

JESÚS GIL
DOMINIC J. WITHERS
Medical Research Council (MRC) London Institute of Medical Sciences
London, United Kingdom
Institute of Clinical Sciences
Faculty of Medicine
Imperial College London
London, United Kingdom

TOM LUEDDE
Department of Gastroenterology
Hepatology and Infectious Diseases
Medical Faculty
University Hospital Düsseldorf
Heinrich Heine University
Düsseldorf, Germany

MATHIAS HEIKENWALDER
Division of Chronic Inflammation and Cancer
German Cancer Research Center (DKFZ)
Heidelberg, Germany

References

1. Burcelin R, et al. Am J Physiol Endocrinol Metab 2002;282:834–842.
2. Anstee Q, et al. Nat Rev Gastroenterol Hepatol 2019;16:411–428.
3. Gallage S, et al. Med 2021;2:505–552.
4. Leone V, et al. Trends Cancer 2021;7:606–623.
5. Wolf M, et al. Cancer Cell 2014;26:549–564.
6. Clapper J, et al. Am J Physiol Gastrointest Liver Physiol 2013;305:G483–G495.
7. Glantz A, et al. et al. Hepatology 2004;40:467–474.
8. Ambros-Rudolph C, et al. Arch Dermatol 2007;143:757–762.
9. Liu Z, et al. BMC Gastroenterol 2018;18:112.
10. Anakk S, et al. Cell Rep 2013;5:1060–1069.

*Authors share co-first authorship.

Abbreviations used in this letter: **ALP, alkaline phosphatase; H-TBA, high total bile acid; L-TBA, low total bile acid; NASH, nonalcoholic steatohepatitis; TBA, total bile acid; WD, Western diet**

Most current article

2352-345X
https://doi.org/10.1016/j.jcmgh.2021.11.012

Received September 6, 2021. Accepted November 29, 2021.

Correspondence
Address correpondence to: Mathias Heikenwälder, PhD, Division of Chronic Inflammation and Cancer, German Cancer Research Center (DKFZ), Im Neuenheimer Feld 280, Heidelberg 69120 Germany. e-mail: m.heikenwaelder@dkfz-heidelberg.de.

Acknowledgments
The authors thank P. Ramadori, S. Prokosch, U. Rothermel, D. Heide, J. Hetzer, T. Machauer, C. Leuchtenberger, F. Müller, and J. Pombo for their support in animal organization and histology-related work. Moreover, the authors also thank the Small Animal Imaging Core Facility German Cancer Research Center (DKFZ) for the magnetic resonance imaging, particularly Dr Viktoria Eichwald for her support in magnetic resonance imaging analysis. The authors also thank the Medical Research Council (MRC) London Institute of Medical Sciences (LMS) Bioinformatics Core Facility (G. Dharmalingam and S. Khadayate) for their support in RNA sequencing analysis. The authors thank R. Kemler and the Developmental Studies Hybridoma Bank for the cytokeratin 19 (CK19) Troma-III antibody. The authors thank M. Vijay-Kumar and members of his laboratory for the helpful discussions.

Funding
Supported by the Medical Research Council grant MC-A654-5QB40 and the Wellcome Trust grant 098565/Z/12/Z (D.J.W.). Also Supported by a European Research Council (ERC) Consolidator grant (HepatoMetaboPath), SFBTR179 project ID 272983813, SFB/TR 209 project ID 314905040, SFBTR1335 project ID 360372040, the Wilhelm Sander-Stiftung, the Rainer Hoenig Stiftung, a Horizon 2020 grant (HEP-CAR), the Rainer Hönig Stiftung, Research Foundation Flanders (FWO) under grant 30826052 (Excellence of Science, EOS, convention MOlecular mechanisms of cellular DEath and Life decisions in Inflammation, Degeneration and Infection, model-IDI), Deutsche Krebshilfe projects 70113166 and 70113167, German-Israeli Cooperation in Cancer Research (German Cancer Research Center-Ministry of Science, Technology & Space, DKFZ-MOST), the Helmholtz-Gemeinschaft, and Zukunftsthema Immunology and Inflammation (ZT-0027) (M.H.).